DOI: 10.1002/chem.200701655

Synthesis and Characterization of a Grapevine Nanostructure Consisting of Single-Walled Carbon Nanotubes with Covalently Attached [60]Fullerene Balls

Wei Wu,[a] Huarui Zhu,[b] Louzhen Fan,*[b] and Shihe Yang*[a]

Abstract: A grapevine nanostructure based on single-walled carbon nanotubes (SWNTs) covalently functionalized with [60]fullerene (C_{60}) has been synthesized and characterized in detail. Investigations into the ball-on-tube carbon nanostructure by ESR spectroscopy indicate a tendency for ground-state electron transfer from the SWNT to the C_{60} moieties. The cyclic-voltammetric response of the nanostructure film exhibits reversible multiple-step electrochemical reactions of the dispersed C_{60}, which are strikingly similar to those of the C_{60} derivatives in solution, but with consistent negative shifts in the redox potential. This results from the covalent linkage of C_{60} to the surfaces of the SWNTs in the form of monomers and manifests the electronic interaction between the C_{60} and SWNT moieties.

Keywords: nanotubes · covalent functionalization · electrochemistry · electronic interaction · fullerenes

Introduction

The discovery of fullerenes, which are solely composed of carbon atoms with fascinating graphitic nanostructures, pioneered a completely new field of research in science and technology. Among the members of the fullerene family, C_{60} and carbon nanotubes (CNTs) have been studied extensively and targeted for applications in many fields due to their unique physical and chemical characteristics as well as mature production technology.[1,2] Furthermore, the combination of these two types of carbon forms has been achieved in different ways, such as encapsulation of C_{60} by single-walled carbon nanotubes (SWNTs) to form the so-called peapods,[3] covalent linkage of C_{60} clusters to the surfaces of CNTs by mechanochemical and electrochemical reactions,[4,5,27] and attachment of C_{60} derivatives through π–π interactions between the surfaces of SWNTs and C_{60}-linked pyrene moieties.[6] However, covalent linkage of well-defined monomeric forms of C_{60} to CNTs, which is more robust and may give rise to novel structures and properties, has not been reported up till now. Herein, we present the first case of the covalent functionalization of SWNTs with a monomeric form of C_{60} by a wet-chemistry method. The product has been characterized in detail and shown to display essentially a grapevine nanostructure with carbon balls attached to carbon tubes (see Figure 1), as opposed to the peapod nanostructure with C_{60} occluded in SWNTs. More-

[a] Dr. W. Wu, Prof. S. Yang
Department of Chemistry
The Hong Kong University of Science and Technology
Clear Water Bay, Kowloon (Hong Kong)
Fax: (+852) 2358-1594
E-mail: chsyang@ust.hk

[b] H. Zhu, Prof. L. Fan
Department of Chemistry, Beijing Normal University
Beijing, 100875 (China)
Fax: (+86) 10-5880-2075
E-mail: lzfan@bnu.edu.cn

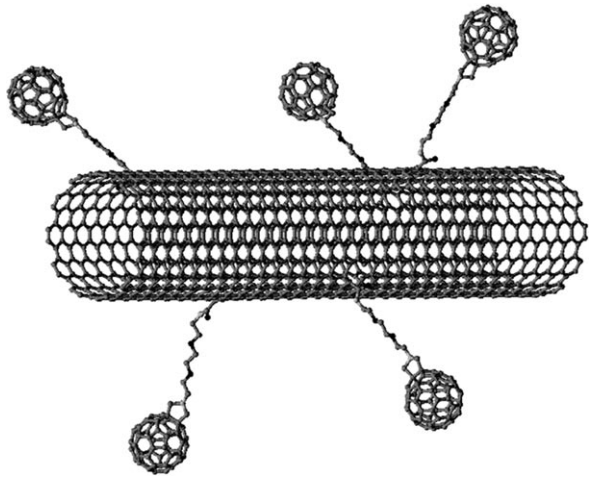

Figure 1. Schematic grapevine structure of SWNTs **3**.

over, the SWNT–C_{60} grapevines immobilized on an electrode exhibit, in addition to the superimposed redox features of the bare SWNTs, reversible electron-transfer reactions of the C_{60} moieties similar to those with the C_{60} derivative in solution, but in marked contrast to those of the C_{60}@SWNT peapods. This shows that the C_{60} moieties are uniformly implanted on the surfaces of the SWNTs by putative covalent linkages.

Results and Discussion

As illustrated in Scheme 1, the C_{60} functionalized SWNTs depicted in Figure 1 (SWNTs **3**) were synthesized by an amidation reaction between the amino group bound to C_{60} (the compound was produced by the neutralization of C_{60} derivative **1**) and oxidized SWNTs (SWNTs **2**, Scheme 1). To ensure the purity of SWNTs **3**, the as-obtained raw product was purified sufficiently by washing with different solvents (e.g. pyridine, chlorobenzene, and methanol) and by separation through centrifugation. The removal of excess C_{60} derivative **1** was monitored by UV/Vis spectroscopy, and the purity of SWNTs **3** was confirmed by TLC (see the Experimental Section for more detailed synthetic procedures). SWNTs **3** were not soluble in any common solvent, which limited their characterization in the solution state. Nevertheless, sufficient proof for the formation of SWNTs **3** was attained by means of FTIR, ultraviolet-visible (UV/Vis), X-ray photoelectron (XPS), Raman, and ESR spectroscopy, as well as secondary-ion mass spectrometry (SIMS) and TEM.

Structural investigation of SWNTs **3** by FTIR spectroscopy revealed an absorption peak at 527 cm^{-1}, which corresponded to the strongest intramolecular F_{1u} mode of C_{60} (inset of Figure 2a) and can be compared with the same but more prominent peak in the FTIR spectrum of the C_{60} derivative **1** shown in Figure 2c.[4,7] This suggests that C_{60} has been attached covalently to SWNTs since the thorough removal of any excess C_{60} derivative **1** was confirmed by UV/Vis spectroscopy. The appearance of an absorption band at 1680 cm^{-1} in the FTIR spectrum of SWNTs **3** revealed the formation of amide carbonyl bonds, which indicates that the linkage between C_{60} molecules and SWNTs has indeed been achieved by amidation. This is consistent with the decrease in the relative absorbance of the carboxylic carbonyl groups bound to the SWNTs (located at 1750 cm^{-1}) after the linkage of C_{60}, with respect to that of the C=C stretch of the SWNTs backbones at 1588 cm^{-1}. Noticeably, an absorbance band at around 1680 cm^{-1} can also be observed in the spectrum of the C_{60} derivative **1** (Figure 2c), but this peak is derived from the carbonyl group of the trifluoroacetate salt formed by the cleavage of the *tert*-butyloxycarbonyl (Boc) group, which can be removed after neutralization and purification treatments.[8]

The formation of SWNTs **3** was further confirmed from the UV/Vis spectrum as shown in Figure 3. Relative to the absorption spectrum of the pristine SWNTs (as-received SWNTs), which show features of the van Hove singularities, the spectra of both SWNTs **2** and **3** are relatively more featureless, due to a substantial sp^2 to sp^3 bonding conversion after the oxidative treatment of the SWNTs.[9,10] The UV/Vis spectrum of a suspension of SWNTs **3** in *o*-dichlorobenzene displays two peaks located at 327 and 430 nm. The peak at 327 nm can be assigned to the allowed $^1T_{1u} \rightarrow {}^1A_g$ transition of C_{60},[11] whereas the peak at 430 nm is the characteristic feature of monofunctionalized C_{60} present in solution in the

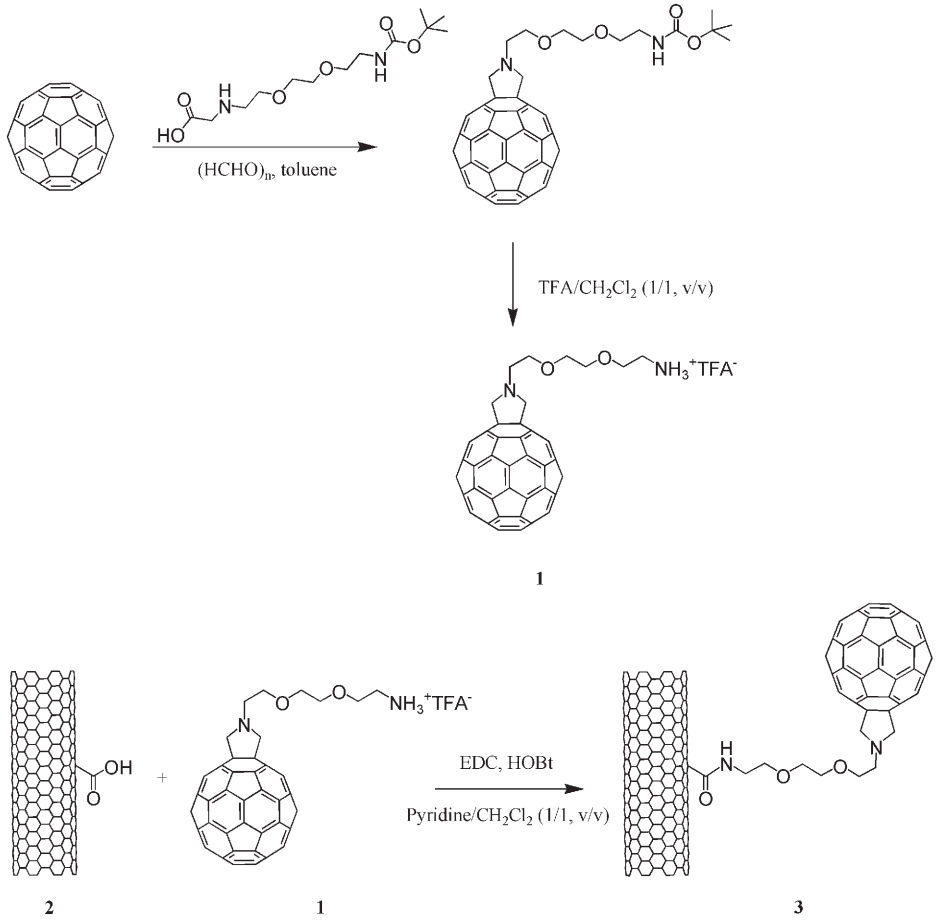

Scheme 1. Reaction scheme for the covalent functionalization of a SWNT with C_{60}. TFA = trifluoroacetic acid, EDC = *N*-(3-dimethylaminopropyl)-*N'*-ethylcarbodiimide hydrochloride, HOBt = 1-hydroxybenzotriazole hydrate.

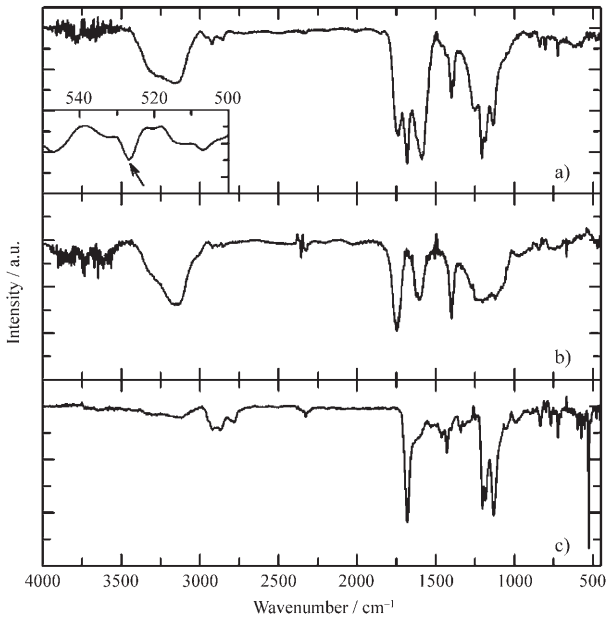

Figure 2. FTIR spectra of a) SWNTs **3** (the inset shows the enlarged F_{1u} mode region, the peak of the F_{1u} mode of C_{60} moieties is denoted by an arrow), b) SWNTs **2**, and c) C_{60} derivative **1**.

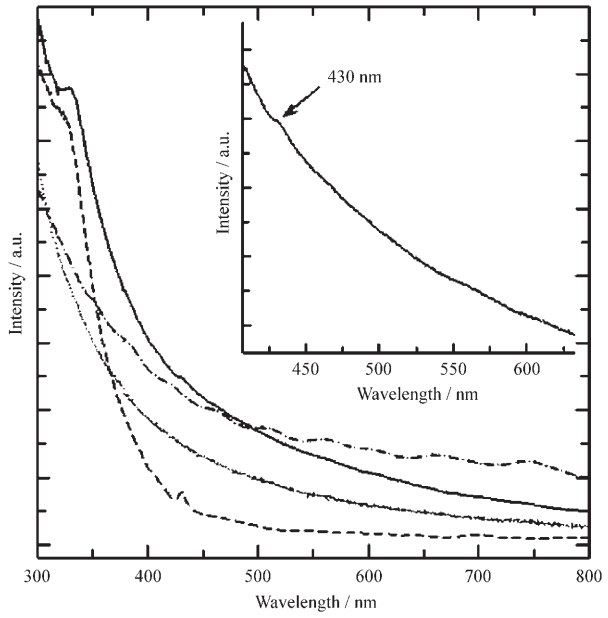

Figure 3. Absorption spectra of SWNTs **3** (——, the inset shows an enlarged region of this spectrum), SWNTs **2** (•••••), pristine SWNTs (–•–•), and C_{60} derivative **1** (-----).

form of monomers (inset of Figure 2),[12] which is in accord with the covalent binding of C_{60} to SWNTs. Remarkably, the monomeric form of the C_{60} molecules on the surfaces of the SWNTs and the absence of aggregations in the suspension of SWNTs **3** suggests the covalent functionalization is quite homogeneous. More directly, the existence of the monomeric form of C_{60} covalently attached to SWNTs can be confirmed by TEM images as vividly shown in Figure 4. The

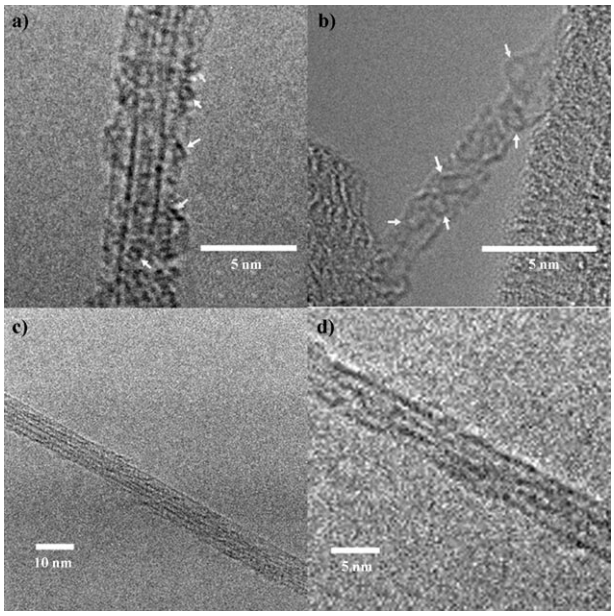

Figure 4. a,b) Typical TEM images of SWNTs **3**, (the arrows denote the C_{60} molecules on the surfaces of the SWNTs). c,d) TEM images of SWNTs **2**.

typical TEM images of SWNTs **2** and **3** (see Figure 4) represent individual/small bundles of SWNTs. In the images of SWNTs **3**, circles (some of them are denoted by white arrows) on the surfaces of SWNTs can be clearly observed. It is reasonable to assume that these circles represent the profiles of the C_{60} molecules simply from their size and shape. In contrast, the SWNTs **2** show only clean and smooth nanotube surfaces.

Raman spectroscopy of SWNTs **3** was also investigated, by comparison with that of SWNTs **2**, C_{60} derivative **1**, and pristine SWNTs, to analyze the effect of the derivatization on the vibrational modes. The results are presented in Figure 5a. In the spectrum of SWNTs **3** (Figure 5), besides the Raman peaks of the tangential mode (G mode) located at 1582 cm^{-1}, the disorder mode (D mode) located at 1347 cm^{-1}, and the radial breathing mode (RBM) located at 170 ~270 cm^{-1},[13] a peak centered at 1458 cm^{-1} can also be observed, which should be assigned to the $A_g(2)$ mode of the C_{60} cage.[14] In addition, it is worth noting that the relative Raman intensity of the D mode of both SWNTs **2** and **3** with respect to their G mode is obviously larger than the corresponding intensity ratio of the pristine SWNTs, which can be ascribed to the increase of structural defects on the SWNTs surfaces induced by the oxidation treatment.[15] This is consistent with the decrease of the UV/Vis absorption features of SWNTs (the van Hove singularities) after the oxidation treatment described above (Figure 3). Figure 6 provides further evidence for the covalent linkage between C_{60} and SWNT moieties by SIMS analysis. A strong peak for C_{60} is clearly observed in the SIMS spectrum of SWNTs **3** in addition to the mass peaks arising from other fragment ions of SWNTs **3**.

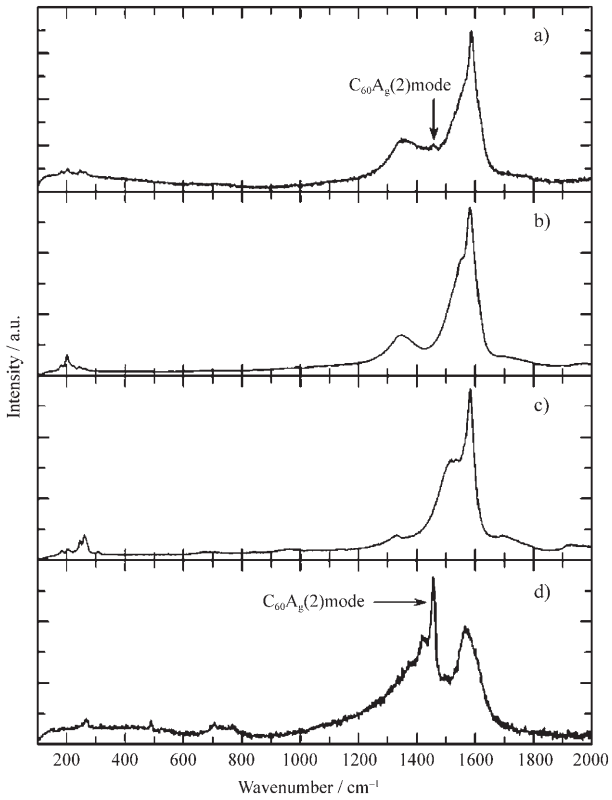

Figure 5. Raman spectra of a) SWNTs **3**, b) SWNTs **2**, c) pristine SWNTs, and d) C_{60} derivative **1**.

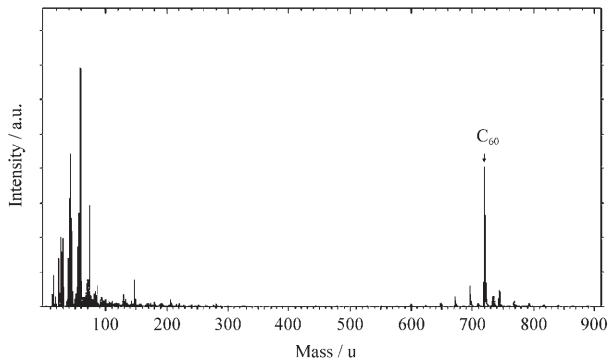

Figure 6. SIMS spectrum of SWNTs **3**.

XPS analysis results for SWNTs **3** are shown in Figure 7a. An N1s peak centered at 399.7 eV is observed and can be fitted to two further line shapes with binding energies of 400.27 and 399.47 eV (inset of Figure 7a), which are ascribable to the pyrrolidine and amide nitrogen atoms, respectively.[16] In contrast, no trace of the N1s peak at the same binding energy can be found in the XPS spectrum of SWNTs **2** (Figure 7b). This serves to verify the formation of the amide bonds in SWNTs **3**. Based on the atomic ratio of C to N determined by XPS, it can be evaluated that one C_{60} molecule is covalently attached for every ~100 carbon atoms of SWNTs **3**. This C_{60} coverage on the SWNTs surfaces appears to be quite high, a fact that is consistent with the TEM images shown in Figure 4.

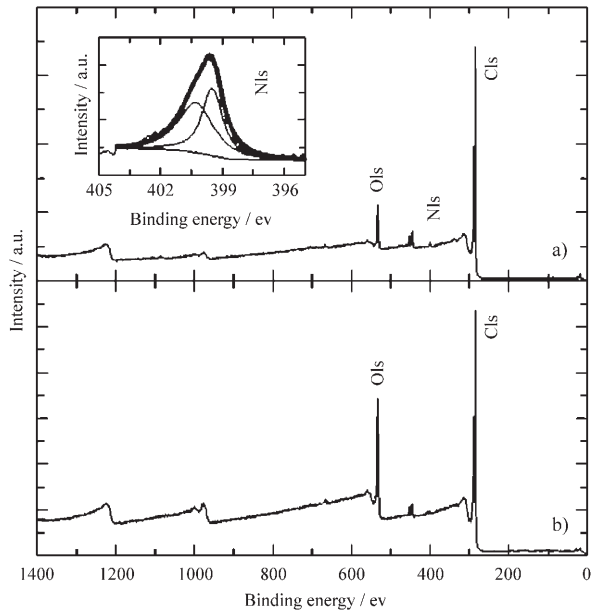

Figure 7. XPS spectra of a) SWNTs **3** (the inset shows a narrow scan spectrum in the N1s region and the corresponding fits) and b) SWNTs **2**.

To understand the electronic interaction between the SWNT and C_{60} moieties of SWNTs **3**, an ESR investigation was carried out. As Figure 8 shows, the ESR spectra of both SWNTs **2** and **3** display a typical first derivative signal with a symmetric partition of the amplitude. The ESR signal from SWNTs **2** that is contributed by the conducting electrons appears at $g \approx 1.9932$ (in which g is the electron g factor) with $\Delta H_{pp} \approx 5$ G (in which ΔH_{pp} is the peak-to-peak

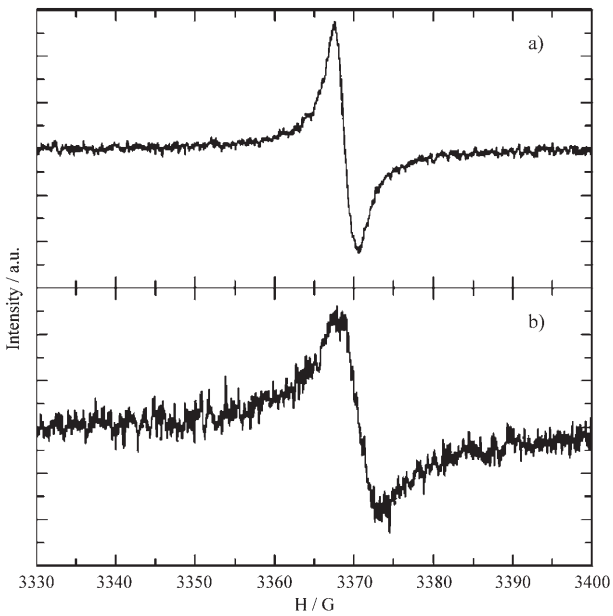

Figure 8. ESR spectrum of a) SWNTs **3** and b) SWNTs **2**.

separation (ESR linewidth)),[17] whereas SWNTs **3** exhibit a relatively narrow ESR signal with a g value of 1.9937 and ΔH_{pp} of 3 G. This distinction should be induced by the electronic interaction between the SWNTs and C_{60} moieties of SWNTs **3**, since both of the ESR spectra were recorded under exactly the same conditions. It is known that C_{60} possesses a stronger electron-withdrawing ability than CNTs,[18] which should conduce to shift the ground-state electron cloud towards C_{60} from the SWNT. However, in our case, no ESR signals from the radical anions of C_{60} derivatives (g value would be in the range of 1.9998 to 2.0010[19]) were found in the ESR spectrum of SWNTs **3**, which indicates only a partial electron transfer or an electron-transfer trend from the SWNT to the C_{60} moiety in SWNTs **3**.

Also, to understand the SWNT–C_{60} interactions, we studied the electronic structure of the grapevine carbon nanomaterial SWNTs **3** by cyclic voltammetry by using the C_{60} derivative **1** as a control. Figure 9a shows cyclic voltamagrams of a film of SWNTs **3**, a film of C_{60} derivative **1**, and **1** dissolved in a mixture of toluene and acetonitrile. Interestingly, well-defined redox responses were observed (——), which resemble those of C_{60} derivative **1** dissolved in an acetonitrile/toluene mixture on a glassy carbon (GC) working electrode (-----), but superimposed on the redox curve of the bare SWNTs with monotonic charge injection over the whole potential range.[20] More specifically, the film of SWNTs **3** exhibits reversible multiple-step electron-transfer reactions corresponding to **1**/**1**$^-$ (-0.98 V), **1**$^-$/**1**$^{2-}$ (-1.33 V), and **1**$^{2-}$/**1**$^{3-}$ (-1.75 V). This is in sharp contrast with the cyclic voltammetric responses of the film of C_{60} derivative **1** in acetonitrile containing 0.1 M tetrabutylammonium hexafluorophosphate ($TBAPF_6$) (see inset of Figure 9a). It is well-known that the redox waves of C_{60} (or its derivatives) films show irreversible behavior (i.e., a large splitting appears between its reduction and re-oxidation waves) because of aggregation and structural rearrangement of the C_{60} molecules.[21] In our case, the irreversible behavior of the film of the C_{60} derivative **1** exhibited in the inset of Figure 9a can also be attributed to the aggregation and structural rearrangement of **1** during cyclic-voltammetric scanning. After C_{60} derivative **1** was chemically linked to the surfaces of the SWNTs to form SWNTs **3**, the film exhibited well-defined redox behavior, with reversible redox waves. This redox behavior resembled that of **1** in solution, which indicates that the sort of aggregation and structural rearrangement observed in the film of **1** has been largely suppressed here, evidently because **1** is now highly dispersed in the uniform matrix of the SWNTs. Moreover, the cyclic-voltammetric responses of the grapevine carbon nanostructure are also different from those of the carbon peapods formed by insertion of C_{60} into the SWNTs, which are actually more analogous to those of empty SWNTs and do not show the distinct redox couples of C_{60}.[3,22] On the other hand, it has been well documented that when an electron-donating molecule such as a porphyrin is covalently attached to C_{60}, a cathodic shift with respect to that of C_{60} is normally observed due to electron transfer between the two moieties.[23,24] In a similar

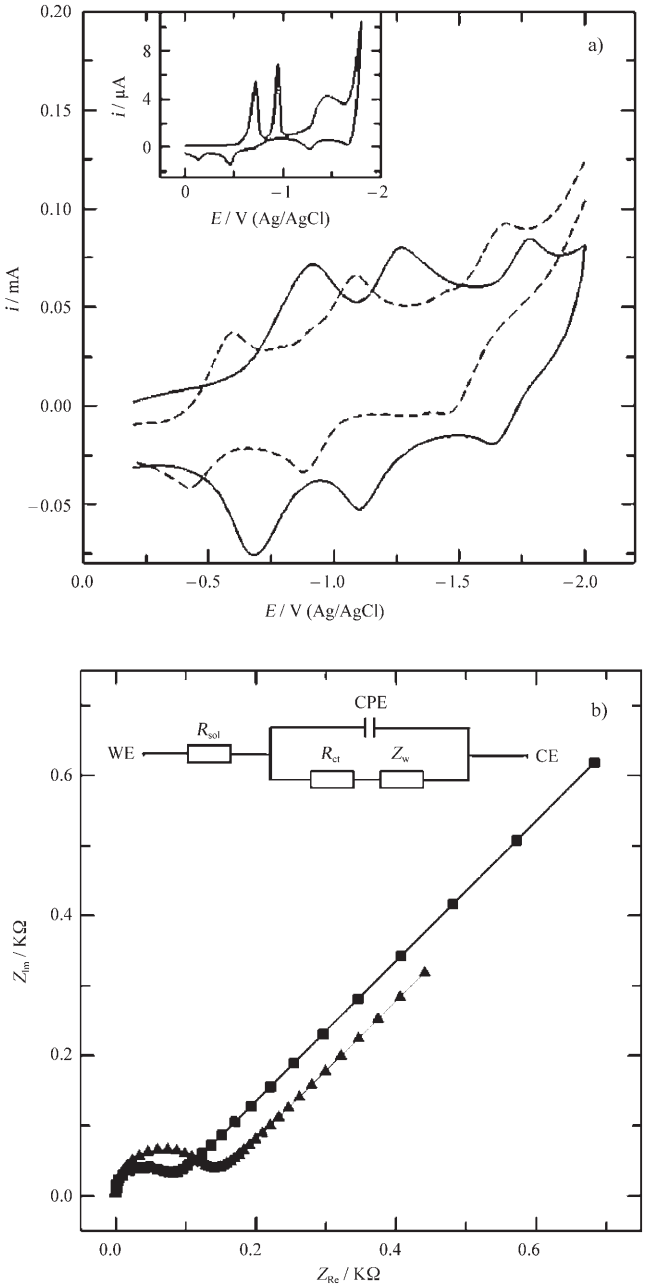

Figure 9. a) Cyclic voltamagrams of a film of SWNTs **3** (——) and a film of **1** (inset) in acetonitrile containing 0.1 mol L^{-1} $TBAPF_6$, and a cylcic voltamagram of **1** (-----) dissolved in a mixture of acetonitrile and toluene (1:4 v/v) containing 0.1 mol L^{-1} $TBAPF_6$ on a GC electrode. b) EIS spectra of SWNTs **3** (▲) and pristine SWNTs (■) in an acetonitrile solution of 5 mM ferrocene. Inset: the equivalent circuit. WE = working electrode, R_{sol} = resistance of solution, CPE = constant phase angle element, R_{ct} = charge-transfer resistance, Z_w = Warburg impedance, CE = counter electrode.

vein, when a SWNT is linked to the C_{60} derivative **1** to form **3**, the electron-donating ability of the SWNT is also expected to yield a cathodic shift as we observed in the film of **3** as listed in Table 1.

From Table 1, it was found that the differences between the reduction waves and corresponding re-oxidation waves

Table 1. Redox potentials of a film of SWNTs **3** and **1** in solution.

	E_r [V][a]			ΔE_p [mV][b]		
	1	2	3	1	2	3
SWNTs **3**	−0.98	−1.33	−1.75	−310	−210	−120
1 (solution)	−0.60	−1.12	−1.63	−101	−104	−110

[a] E_r = Reduction wave potentials versus Ag/AgCl. [b] $\Delta E_p = E_r - E_o$, in which E_o is the corresponding re-oxidation wave potential.

(ΔE_p) for SWNTs **3** are much larger than those for **1** in solution, which can be taken as an indication of the conductivity decrease of the SWNTs due to functionalization. To test for conductivity changes in the SWNTs due to functionalization, we relied on electrochemical impedance spectroscopy (EIS) measurements. The EIS results for SWNTs **3** and pristine SWNTs are presented in Figure 9b. The probe was ferrocene in an acetonitrile solution and the equivalent Randles circuit, shown in the inset of Figure 9b, was used to analyze the EIS spectra. The semicircle part at high frequency corresponds to a limited electron-transfer process. It can be seen that the charge-transfer resistance (R_{ct}) value for the SWNTs **3** electrode (122.8 Ω) is much higher than that for the pristine SWNTs electrode (27.17 Ω), and this proves that the conductivity of SWNTs will decrease after the oxidation reaction that leads to the sp^2 to sp^3 bonding conversion of SWNTs.

In light of these results, some deductions can be made. First, the C_{60} molecules are uniformly implanted on the surfaces of the SWNTs in the form of monomers as already concluded above, which results in the characteristic redox waves of the C_{60} derivative with sequential and reversible electrochemical reactions. Second, with the SWNTs **3** electrode, all of the observed reduction wave potentials shift significantly in the negative direction relative to that of the C_{60} derivative **1**. To explain this observation, two possibilities can be considered. First, the negative-potential shift is ascribable to the electron-transfer trend from SWNT to C_{60} moieties in the ground state,[25] as inferred from the ESR results. Second, one can also attribute the negative potential shift to the covalent bonding of C_{60} to the SWNT framework. One would expect that the covalent bonding of functional groups to the SWNTs disrupts the π-electronic structure of the tubular framework,[26] because the participating carbon atoms of the SWNTs are converted from the sp^2 to sp^3 bonding pattern as already discussed above. This in turn would decrease the conductivity of the SWNTs and weaken the electronic communication between C_{60} and the underlying GC electrode. As a result, it would be more difficult for C_{60} in SWNTs **3** to receive electrons than in the organic solution and this explains the significant negative shift of the reduction potentials of SWNTs **3** on the GC electrode. To sum up, the electrochemical results, above all, point to the uniform covalent attachment of C_{60} to the outer surfaces of SWNTs.

Conclusion

A grapevine nanostructure based on CNTs covalently functionalized with C_{60} has been synthesized and thoroughly characterized. The cyclic-voltammetric responses of the grapevine-nanostructure film remarkably resemble that of the C_{60} derivative in solution and exhibit reversible multiple-step electrochemical reactions, which reflect the covalent attachment of the C_{60} molecules to the surfaces of SWNTs in the form of monomers. The results of ESR spectroscopy reveal the ground-state electron-transfer trend from SWNT to C_{60} moieties in the grapevine nanostructure. Such a robust grapevine carbon nanostructure allows comparisons of the redox responses of C_{60} with those in the peapods and in solutions, and provides a platform for dispersing C_{60} molecules with potential applications in wide-ranging fields such as biosensors.

Experimental Section

General: SWNTs were purchased from Carbon Nanotechnologies, Inc., USA. [60]Fullerene and HOBt were purchased from International Laboratory, USA. 2,2′-(Ethylenedioxy)diethylamine, di-*tert*-butyl dicarbonate, and EDC were obtained from Fluka. All other reagents and solvents were obtained from commercial suppliers and used without further purification.

UV/Vis absorption spectra were recorded on a Perkin–Elmer Lambda 900 UV/VIS/NIR double beam spectrometer. FTIR spectra were collected by using a Perkin–Elmer Spectrum One spectrometer. The samples were homogeneously dispersed in KBr pellets. Raman spectra were measured on a MicroRaman System RM3000 spectrometer with an excitation wavelength of 514.5 nm (Ar laser). TOF SIMS analyses were performed on a TOF SIMS V. XPS analyses were carried out on a Surface Analysis PHI5600 instrument. TEM observations were conducted on a JEOL2010F microscope operating at 200 kV. ESR spectroscopy experiments were carried out by using a JEOL JES-TE-200 ESR spectrometer. All the samples were measured as powder at 298 K.

The electrochemical measurements were performed with a three-electrode system. The GC (3 mm diameter) electrodes or the SWNT **2/3** modified GC electrodes were used as the working electrodes. A Pt-wire electrode served as the counter electrode, and a Ag/AgCl electrode was used as the reference electrode. All of the electrochemical experiments were carried out by using CHI610B (Austin, USA) in acetonitrile or a mixture of toluene and acetonitrile, containing 0.1 M $TBAPF_6$ (supporting electrolyte) that was thoroughly deaerated with high-purity nitrogen before use at ambient temperature. Cyclic voltamagrams were measured at a scan rate of 100 $mV s^{-1}$. To clean the GC electrode, the surface of the GC electrode was polished with chamois leather soaked with alumina slurry, ultrasonically cleaned in toluene for a few minutes, and dried in a high-purity nitrogen stream. For the preparation of the SWNTs **2/3** modified GC electrodes, a suspension of the corresponding SWNTs in toluene (0.1 $mg mL^{-1}$) was prepared. The GC electrode was then cast with 15 μL of the obtained SWNTs suspension and dried in air before use. The modified electrodes were very stable throughout the measurement process.

Synthesis of SWNTs 3: The C_{60} derivative **1** was synthesized by following the reported procedures (Scheme 1).[8] Oxidized SWNTs **2** (3 mg) and a solution of EDC (28.8 mg) and HOBt (20.3 mg) in dichloromethane (3 mL) were added to a solution of C_{60} derivative **1** (3.4 mg) in pyridine (3 mL). The resulting black mixture was stirred at room temperature overnight. The solid component was separated by centrifugation and washed with pyridine, chlorobenzene, and methanol successively. The removal of excess C_{60} derivative **1** was monitored by UV/Vis spectroscopy

and the purity of the resulting SWNTs **3** was confirmed by TLC. After evaporation of the solvent, SWNTs **3** were obtained as a black solid (4.3 mg).

Acknowledgements

This work is supported by grants administrated by the UGC of Hong Kong (NNSFC-RGC: N HKUST604/04, RGC: 604206, HKUST: HIA05/06.SC02), and the National Natural Science Foundation of China (20773015).

[1] a) J. Shinar, Z. V. Vardeny, Z. H. Kafafi, *Optical and Electronic Properties of Fullerenes and Fullerene-Based Materials*, Marcel Dekker, New York, **2000**, pp 21–292; b) D. M. Guldi, N. Martin, *Fullerenes: From Synthesis to Optoelectronic Properties*, Kluwer Academic, Dordrecht, (The Netherlands), **2002**, pp 137–293; c) E. Dagotto, *Science* **2001**, *293*, 2410–2411; d) R. C. Haddon, A. S. Perel, R. C. Morris, T. T. M. Palstra, A. F. Hebard, R. M. Fleming, *Appl. Phys. Lett.* **1995**, *67*, 121–123.

[2] a) S. Niyogi, M. A. Hamon, H. Hu, B. Zhao, P. Bhowmik, R. Sen, M. E. Itkis, R. C. Haddon, *Acc. Chem. Res.* **2002**, *35*, 1105–1113; b) J. L. Bahr, J. M. Tour, *J. Mater. Chem.* **2002**, *12*, 1952–1958; c) D. Tasis, N. Tagmatarchis, A. Bianco, M. Prato, *Chem. Rev.* **2006**, *106*, 1105–1136; d) W. Wu, S. Zhang, Y. Li, J. X. Li, L. Q. Liu, Y. J. Qin, Z. X. Guo, L. M. Dai, C. Ye, D. B. Zhu, *Macromolecules* **2003**, *36*, 6286–6288; e) W. Wu, S. Wieckowski, G. Pastorin, M. Benincasa, C. Klumpp, J.-P. Briand, R. Gennaro, M. Prato, A. Bianco, *Angew. Chem.* ***2005****, 117, 6516–6520; Angew. Chem. Int. Ed.* **2005**, *44*, 6358–6362; f) W. Wu, H. Zhu, L. Fan, D. Liu, R. Renneberg, S. Yang, *Chem. Commun.* **2007**, 2345–2347.

[3] a) L. Kavan, L. Dunsch, H. Kataura, *Chem. Phys. Lett.* **2002**, *361*, 79–85; b) L. Kavan, L. Dunsch, H. Kataura, A. Oshiyama, M. Otani, S. Okada, *J. Phys. Chem. B* **2003**, *107*, 7666–7675.

[4] X. Li, L. Liu, Y. Qin, W. Wu, Z. Guo, L. Dai, D. Zhu, *Chem. Phys. Lett.* **2003**, *377*, 32–36.

[5] a) H. Zhang, L. Fan, Y. Fang, S. Yang, *Chem. Phys. Lett.* **2005**, *413*, 346–350; b) H. Zhang, L. Fan, S. Yang, *Chem. Eur. J.* **2006**, *12*, 7161–7166.

[6] D. M. Guldi, E. Menna, M. Maggini, M. Marcaccio, D. Paolucci, F. Paolucci, S. Campidelli, M. Prato, G. M. A. Rahman, S. Schergna, *Chem. Eur. J.* **2006**, *12*, 3975–3983.

[7] W. Krätschmer, L. D. Lamb, K. Fostiropoulos, D. R. Huffman, *Nature* **1990**, *347*, 354–358.

[8] K. Kordatos, T. D. Ros, S. Bosi, E. Vázquez, M. Bergamin, C. Cusan, F. Pellarini, V. Tomberli, B. Baiti, D. Pantarotto, V. Georgakilas, G. Spalluto, M. Prato, *J. Org. Chem.* **2001**, *66*, 4915–4920.

[9] J. Chen, M. A. Hamon, H. Hu, Y. Chen, A. M. Rao, P. C. Eklund, R. C. Haddon, *Science* **1998**, *282*, 95–98.

[10] D. Bonifazi, C. Nacci, R. Marega, S. Campidelli, G. Ceballos, S. Modesti, M. Meneghetti, M. Prato, *Nano Lett.* **2006**, *6*, 1408–1414.

[11] a) Z. Gasyna, P. N. Schatz, J. P. Hare, T. J. Dennis, H. W. Kroto, R. Taylor, D. R. M. Walton, *Chem. Phys. Lett.* **1991**, *183*, 283–291; b) S. Leach, M. Vervloet, A. Desprès, E. Bréheret, J. P. Hare, T. J. Dennis, H. W. Kroto, R. Taylor, D. R. M. Walton, *Chem. Phys.* **1992**, *160*, 451–466.

[12] G. Angelini, P. D. Maria, A. Fontana, M. Pierini, M. Maggini, F. Gasparrini, G. Zappia, *Langmuir* **2001**, *17*, 6404–6407.

[13] a) J. M. Holeden, Z. Ping, X. X. Bi, P. C. Eklund, S. J. Bandow, R. A. Jishi, K. Daschowdhury, G. Dresselhaus, M. S. Dresselhaus, *Chem. Phys. Lett.* **1994**, *220*, 186–191; b) A. M. Rao, E. Richter, S. Bandow, B. Chase, P. C. Eklund, K. A. Williams, S. Fang, K. R. Subbaswamy, M. Menon, A. Thess, R. E. Smalley, G. Dresselhaus, M. S. Dresselhaus, *Science* **1997**, *275*, 187–191; c) A. Jorio, G. Dresselhaus, M. S. Dresselhaus, M. Souza, M. S. S. Dantas, M. A. Pimenta, A. M. Rao, R. Saito, C. Liu, H. M. Cheng, *Phys. Rev. Lett.* **2000**, *85*, 2617–2620.

[14] D. S. Bethune, G. Meijer, W. C. Tang, H. J. Rosen, *Chem. Phys. Lett.* **1990**, *174*, 219–222.

[15] D. Bonifazi, C. Nacci, R. Marega, S. Campidelli, G. Ceballos, S. Modesti, M. Meneghetti, M. Prato, *Nano Lett.* **2006**, *6*, 1408–1414.

[16] a) F. Cecchet, S. Rapino, M. Margotti, T. D. Ros, M. Prato, F. Paolucci, P. Rudolf, *Carbon* **2006**, *44*, 3014–3021; b) G. Beamson, D. Briggs, *High Resolution XPS of Organic Polymers - The Scienta ESCA Database*, Wiley, Chichester, (UK) **1992**.

[17] a) Y. Chen, J. Chen, H. Hu, M. A. Hamon, M. E. Itkis, R. C. Haddon, *Chem. Phys. Lett.* **1999**, *299*, 532–535; b) P. Petit, E. Jouguelet, J. E. Fischer, A. G. Rinzler, R. E. Smalley, *Phys. Rev. B* **1997**, *56*, 9275–9278.

[18] a) M. Alvaro, P. Atienzar, P. D. L. Cruz, J. L. Delgado, V. Troiani, H. Garcia, F. Langa, A. Palkar, L. Echegoyen, *J. Am. Chem. Soc.* **2006**, *128*, 6626–6635; b) D. A. Britz, A. N. Khlobystov, *Chem. Soc. Rev.* **2006**, *35*, 637–659.

[19] a) V. V. Yanilkin, V. P. Gubskaya, V. I. Morozov, N. V. Nastapova, V. V. Zverev, E. A. Berdnikov, I. A. Nuretdinov, *Russ. J. Electrochem.* **2003**, *39*, 1147–1165; b) S. Fukuzumi, H. Mori, T. Suenobu, H. Imahori, X. Gao, K. M. Kadish, *J. Phys. Chem. A* **2000**, *104*, 10688–10694.

[20] a) L. Kavan, P. Rapta, L. Dunsch, M. J. Bronikowski, P. Willis, R. E. Smalley, *J. Phys. Chem. B* **2001**, *105*, 10764–10771; b) E. Frackowiak, F. Beguin, *Carbon* **2001**, *39*, 937–950.

[21] a) C. Jehoulet, Y. O. Obeng, Y. T. Kim, F. Zhou, A. J. Bard, *J. Am. Chem. Soc.* **1992**, *114*, 4237–4247; b) P. Janda, T. Krieg, L. Dunsch, *Adv. Mater.* **1998**, *10*, 1434–1438.

[22] L. Cai, J. L. Bahr, Y. Yao, J. M. Tour, *Chem. Mater.* **2002**, *14*, 4235–4241.

[23] S. Fukuzumi, K. Ohkubo, H. Imahori, J. Shao, Z. Ou, G. Zheng, Y. Chen, R. K. Pandey, M. Fujitsuka, O. Ito, K. M. Kadish, *J. Am. Chem. Soc.* **2001**, *123*, 10676–10683.

[24] S. Nagase, K. Kobayashi, T. Akasaka, T. Wakahara, in *Fullerenes: Chemistry, Physics and Technology* (Eds.: K. M. Kadish, R. S. Ruoff), Wiley, New York, **2000**, pp. 15–26.

[25] M. S. Strano, C. A. Dyke, M. L. Usrey, P. W. Barone, M. J. Allen, H. Shan, C. Kittrell, R. H. Hauge, J. M. Tour, R. E. Smalley, *Science* **2003**, *301*, 1519–1522.

[26] A. Gouloumis, S.-G. Liu, Á. Sastre, P. Vázquez, L. Echegoyen, T. Torres, *Chem. Eur. J.* **2000**, *6*, 3600–3607.

[27] *Note added in proof*: A recent and related paper on a covalent adduct of C_{60} and CNTs has come to our attention: J. L. Delgado, P. de la Cruz, A. Urbina, J. T. López Navarrete, J. Casado, F. Langa, *Carbon.* **2007**, *45*, 2250.

Received: October 20, 2007
Revised: February 20, 2008
Published online: May 19, 2008

Reference [27] has been added since the online publication of this article.

